2016

Improved Systems For On-Site Raman Measurements

William Joshua Huntington
University of South Carolina

IMPROVED SYSTEMS FOR ON-SITE RAMAN MEASUREMENTS

by

William Joshua Huntington

Bachelor of Science
University of South Carolina, 2012

Submitted in Partial Fulfillment of the Requirements

For the Degree of Master of Science in

Chemistry

College of Arts and Sciences

University of South Carolina

2016

Accepted by:

S. Michael Angel, Director of Thesis

John Ferry, Reader

Lacy Ford, Senior Vice Provost and Dean of Graduate Studies

DEDICATION

I dedicate this work to my family. Mom thank you for raising me to be who I am, Ryan I could not hope for a better brother or friend, and Dad thank you for what you taught me and I wish you could have been here to see me succeed. Finally I dedicate this work to my wife Kayla. I love you more than words could ever express and look forward to a long life with you.

ACKNOWLEDGEMENTS

I must first and foremost thank my family, my mother Darlene, my father Stoney, and my brother Ryan, for their love and support throughout my life. Without you all I would not be here today. I was lucky to have encouragement and opportunities to learn a multitude of skills and values that made me into the man I am today. Thank you for everything you have done for me and I hope to continue making you proud.

I would like to thank Dr. S. Michael Angel for everything that I have learned in my time with the Angel group. He took a chance with me and taught me how to observe and question what is happening around me, molding me into the scientist I am today. I am truly grateful for everything he has taught me. He also gave me the opportunity to work with a group of colleagues who have had a major impact on my life. I would like to thank the current and former members of the Angel group, Nirmal Lamsal, Alicia Strange (Fessler), Joseph Bonvallet, and Patrick Barnet, for being there when I needed help and for being my friends when I needed someone to talk to.

I would like to give my utmost thanks to my amazing and supporting wife Kayla. I have known you for my entire adult life and without a doubt you are the reason I am who I am. I have experienced the greatest moments and worst tragedies in my life with you and you have been by my side for every minute of it with love and support to help me through it all. You have given me the courage and support to pursue my dreams and ambitions and I could never thank you enough for everything you do for me.

ABSTRACT

The need to development lightweight miniature sensors for spectrometers for use in hazardous environments such as war zones, industrial settings, and space exploration is ever growing. This thesis will present studies aimed at improving Raman instruments for such applications by reducing the size, weight, and power consumption of the instrument. The two methods described here include the utilization of a light emitting diode (LED) source for Raman spectroscopy and a new type of Raman gas sensor.

Chapter one describes a new Raman spectrometer that utilizes an LED for Raman excitation coupled to the SHRS. LEDs are highly divergent broadband , extended light sources that are not typically suitable for Raman measurements. In this work a broadband LED is optically filtered and the light is focused onto various solid and liquid samples where the large field of view of the SHRS is fully utilized to collect a large fraction of the Raman scattered light. The coupling of the SHRS with LED excitation shows great promise for the full utilization of LED excitation and provides great potential for spectrometer miniaturization and reduction of instrument size, weight, and power consumption.

Chapter two describes two new Raman gas cells. The first method couples a multi-pass capillary cell (MCC) to the newly developed spatial heterodyne Raman spectrometer (SHRS). The SHRS's large field of view allows for directly coupling the MCC to the spectrometer without a fiber optic while maintaining a signal to noise ratio

equivalent to the results recorded using fiber optically coupled MCC devices. The second method involves new hollow waveguide (HWG) designs, and a new gas chamber coupled to a dispersive Raman spectrometer with a new type of fiber optic Raman probe.

TABLE OF CONTENTS

LIST OF FIGURES

CHAPTER 1

Spatial Heterodyne Raman Spectrometer with a Light Emitting Diode Excitation Source

1.1 Abstract

The use of LED light sources offers the potential to decrease the size, weight, and power consumption of Raman instruments. These considerations are particularly important for instruments that may be used in planetary exploration. For many Raman applications the output power of LED sources is sufficiently high, but the emission bandwidth is much broader than most Raman bands. Optical bandpass filters can be used to decrease the line width of the LED source, but at the expense of transmitted power. Dispersing the LED emission using a diffraction grating has also been demonstrated, by focusing the dispersed light onto the sample, so that the excitation wavelength changes across it, and using an imaging detector to collect the Raman scattered light and reconstruct the Raman spectrum. A difficulty with this approach is low light throughput. The optical extent (i.e. etendue) of high power LED sources is much larger than traditional spectrometers, making it difficult to efficiently collect Raman scattered light from an illuminated sample region with a dispersive spectrometer. The spatial heterodyne Raman spectrometer (SHRS) has a wide acceptance angle and no slit (i.e., large etendue), allowing much more efficient collection of Raman scattered light using LED excitation.

This paper demonstrates the use of a red wavelength LED as a Raman excitation source with the SHRS.

1.2 Introduction

A few attempts at using light-emitting diodes (LEDs) as Raman excitation sources have been made with various degrees of effectiveness. These studies tend to focus on a proof of concept approach measuring only broad Raman bands that are well separated far from other bands or using the LEDs for shifted-excitation Raman difference spectroscopy (SERDS) to eliminate sample flourescence.[1-5] LEDs are inexpensive, small, robust, have long lifetimes, and low power consumption thus making them ideal for low-cost, lightweight, and efficient spectroscopic instruments. However LEDs come with some disadvantages. LEDs are broadband light sources, which limits the potential resolution of the Raman spectra and limits how well the LED can be focused. There are various established methods for limiting the bandpass of the LED but all suffer from low light throughput.

The spatial heterodyne Raman spectrometer (SHRS) is a compact, high resolution interferometer with a wide acceptance and a large etendue allowing efficient collection of Raman scattered light. The SHRS is based on a stationary diffraction grating, heterodyne interferometer first introduced by Harlander and later modified by Gomer et al for visible Raman measurements.[6-8] There is no entrance slit to limit light entering the spectrometer and the resolution is not strongly tied to aperture size. Heterodyning in the interferometer allows for high spectral resolution to be achieved with a relatively small number of

samples, fixed by the number of horizontal pixels on the imaging detector. The large entrance aperture and wide accepting angle provides high light throughput and allows large spots sizes to be used on the sample without light loss or the loss of spectral resolution. This is key feature that the SHRS will allow for the collection of the entire LED spot size on the sample without a complex optical arrangement or light loss.

1.3 Experimental

The experimental setup is shown schematically in Fig. 1.1 a red LED (Thor Labs M625L3) with a peak wavelength ~630 nm and 15 nm FWHM is used. A 25 mm aspheric condenser lens with a 20 mm focal length is used to collimate the LED. The collimated beam transmits through two 1 nm bandpass laser line filters (Thor Labs, FL632.8-1) centered at 632.8 nm. The filtered light is then focused to a ~4 mm spot with ~4 mW of power on the sample in a quartz cuvette with an f/1 lens. The Raman scattered light is collected at 45 ° using an f/4 collection lens to collimate the scattered light. The collimated light passes through a 632.8 nm notch filter (Edmund optics, 67-111) and a 650 longpass filter (Thor Labs, FEL0650) into the entrance aperture of the SHRS.

The collimated beam is separated in the arms of the SHRS by a 25 mm beamsplitter (Thor Labs, CM1-BS013) onto a 25 mm, 150 grooves/mm grating. The gratings are imaged with a magnification of ~1 onto a liquid nitrogen cooled charge-coupled detector (CCD) with 1024x256 pixel (Princeton Instrument, Model LN/CCD-1024EUV), using a 86 mm focal length camera lens (Nikon AF Nikkor). CCD fringe images were recorded using Winspec software provided with the detector. Apart from the fringe image, three additional images were acquired for each spectrum. These

additional images were sometimes used for background correction of the fringe images. Fourier transforms of the fringe images were performed using the fast Fourier transform (FFT) function in Matlab. Each spectrum was apodized using a Hamming function to reduce ringing effects in the spectral baseline. The Raman spectra were calibrated by locating the position of known Raman bands and using a polynomial fit. No flat field or instrument efficiency corrections, phase correction, smoothing, sharpening, or any other post-processing such as zero filling was used for any of the data presented in this paper.

1.4 Results and Discussion

1.4.1 Working principal of the SHRS

The operation of the SHRS has been previously described and is only briefly presented here.[8-10] During SHRS measurements, the scattered Raman light is collected, collimated and passed through the interferometer entrance aperture and divided into two coherent beams by the 50/50 fused silica cube beamsplitter, as shown in Fig. 1 The two beams are then diffracted by the diffraction gratings at an angle that depends on the wavelength as:

$$n\,\lambda = d(sin\alpha + sin\beta) \qquad (1)$$

Where *n* is diffraction order, λ is the wavelength of interest, d is diffraction grating groove density, and α and β are the angles of incidence and diffraction. Heterodyning in the interferometer is achieved by setting the grating angles in such a way that the light at

wavelength (λ_L) or wavenumber (σ_L) is exactly retroreflected back along the same beam path. For 1st order diffraction,

$$\theta_L = sin^{-1}(\lambda/2d) \qquad (2)$$

where θ_L is the Littrow wavelength (or wavenumber, σ_L) where light is exactly retroreflected from the gratings. For any wavenumber other than Littrow, the diffracted beams leave the gratings at an angle, resulting in crossed wavefronts, generating an interference pattern, which produces a series of wavelength dependent fringes on the detector. The number of fringes produced on the detector is given by Eqn. 3, where *f* is in fringes/cm.[7,11,12] The intensity of fringes obtained as a function of detector position, *x*, is given by Eqn. 4, [7,11,12] where *B(σ)* is the input spectral intensity at wave number σ. The Fourier transform of *I(x)* yields the Raman spectrum:

$$f = 4\,(\sigma - \sigma_L)\,\tan\theta_L \qquad (3)$$

$$I(x) = \int_0^\infty B(\sigma)[1 + \cos\{8\pi(\sigma - \sigma_L)\,x\tan\theta_L\}]\,d\sigma \qquad (4)$$

1.4.2 LED spot size and SHRS area viewed

As seen in Fig. 1.2A the LED spot size on the sample is accurately measured by focusing the LED onto a power meter. A razor edge is attached to a translational stage so as to be moved in consistent 0.25 mm increments blocking the power meter. By recording the LED power in consistent increments as the razor edge is moved across the power meter a curve can be generated that gives an accurate measure of the LED spot size. The use of an f/1 lens to focus the LED produces a spot size of ~4 mm. In this case

the spot size on the sample is approximately the same size as the LED element itself. Figure 1.2B shows how much of the spot focused on the sample is collected by the SHRS. With the f/4 collection lens in this setup an area viewed of ~3.5 mm is calculated. In order to check this calculation a razor edge is used to block the excitation spot on a sulfur sample and the Raman peak intensity is measured as the razor edge is moved across the sample in 0.5 mm increments. This generates a curve which can be used to determine the actual area viewed by the SHRS. A collected spot size of ~3-4 mm is measured which agrees well with the calculated size. The large acceptance angle and area viewed by the SHRS is used to the fullest extent when measuring Raman spectra with an excitation source like an LED. A dispersive system with a small entrance slit, would have a small field of view and would not be suitable to use with a large LED.

1.4.3 Raman measurement with LED excitation

Figure 1.3 displays results comparing LED excitation with laser excitation. The LED data was collected with ~4 mW at 60 s acquisition while the laser data was collected with ~1 W at 10 s acquisition.[12] Fig. 1.3A shows the 600 cm^{-1} to 1700 cm^{-1} region of the Raman spectra of NH_4NO_3. In order to plot the LED and laser data, collected with different instruments, on the same scale the LED intensities are multiplied by 600. It is clear that both the LED and laser show the prominent Raman band at 1043 cm^{-1} due to the NO_3^- symmetric stretching mode. The LED excited Raman full width half max (FWHM) is approximately 27 cm^{-1} which is limited due to the 26 cm^{-1} wide bandpass filter used to limit the LED excitation wavelength. Fig. 1.3B shows the 400 cm^{-1} to 1400 cm^{-1} region of the Raman spectra of $KClO_4$. In order to plot the LED and laser data on the same scale the LED intensities are multiplied by 1100. The prominent Raman band at

942 cm^{-1} due to the ClO_4^- vibrational mode is clearly distinguished with both LED and laser excitation. The resolution of the LED data is again limited by the bandpass filters FWHM. With the LED excitation of $KClO_4$ the relative intensities of the peaks do not agree with the laser excited data or what is reported.[9,10,12] The low LED excitation power in combination with the dampening of the Raman signal for bands further away from the Littrow positon contribute to the difference show in the relative intensities. This is the first direct comparison of LED and laser Raman excitation of solid samples. All current literature focuses on looking at broad band Raman lines, specifically the O-H stretching lines of methanol, water, and ethanol[1-5]. The use of important solid samples, specifically solid samples with Raman features close together and close to the excitation wavelength, show the true potential to use LED sources for small Raman instruments.

Figure 1.4 shows LED spectra of some common solid samples chosen to showcase LED excitation. All samples were collected with the Littrow set at ~585 cm^{-1} and with ~4 mW of LED power at 60 s acquisition time. The samples are offset for clarity. The prominent Raman bands of Na_2CO_3 at 1087 cm^{-1} (CO_3^- vibrational mode), $(NH_4)_2SO_4$ at 970 cm^{-1} (S-O symmetric stretching), and urea at 1013 cm^{-1} (C-N vibrational mode) are clearly observed. The urea sample gives a unique opportunity with a solid sample to showcase a peak that falls below the Littrow wavelength. The peak labeled A is the 550 cm^{-1} band showing up in the spectra even though it falls below the Littrow wavelength. The solid samples shown in Fig. 1.3 And Fig.1.4 were chosen in order to showcase that LED excitation can be used for more than wideband, highly scattering liquid samples.[1-5] LED excitation coupled with a SHRS can be a powerful tool

for measuring very important industrial and geological solid samples with a potentially very small Raman instrument.

Figure 1.5 shows LED spectra of two common liquid samples chosen to showcase LED excitation narrow bands relatively close together. All samples were collected with the Littrow set at ~585 cm^{-1} and with ~4 mW of LED power at 300 s acquisition. The samples are offset for clarity. The cyclohexane bands at 803 cm^{-1} and 1029 cm^{-1} are clearly distinguished and the relative intensities agree with the literature. The toluene bands at 787 cm^{-1} and 1005 cm^{-1} are clearly distinguished but much like $KClO_4$ shown previously the relative intensities do not match with reported spectra.[9,10,12] Once again this is most likely due to the low Raman signal and its distance from the Littrow wavelength. Toluene much like urea gives a unique opportunity to showcase a peak that falls below the Littrow wavelength. The peak labeled A is the 522 cm^{-1} band showing up in the spectra even though it falls before the Littrow position. These samples were chosen in order to showcase some liquid samples that have not previously been measured by LED excitation and much like the solid samples to showcase that LED excitation can be useful when bands are relatively narrow, close to each other, and close to the excitation wavelength.[1-5]

Figure 1.6 shows Raman spectra of DMSO collected at two different Littrow positions in order to showcase the high resolution of the SHRS with LED excitation and how a full spectrum of a solution can be collected by moving the Littrow position. The strong Raman bands at 670 cm^{-1} and 700 cm^{-1} are not fully separated, with the 700 cm^{-1} band showing as a shoulder on the 670 cm^{-1} band, but this is to be expected when the

LED itself is limited by ~26 cm^{-1} wide bandpass filter. The key feature here is that the 2913 cm^{-1} and 2997 cm^{-1} bands are fully resolved which is not shown in the current literature.[1-5]

1.5 Conclusions

For the first time a SHRS is coupled with LED excitation to measure Raman spectra of solid and liquid samples. The SHRS proves to the well suited for LED excited Raman measurements. The large field of view of the SHRS matches well with the large spot size produced by an LED excitation source. However the current work is limited by low LED power, resulting from poor filter transmittance of the broad bandwidth LED source. Future work will focus on using a second SHS to modulate the LED source, which would increase the LED power on the sample, without loss of spectral resolution.

1.6 Acknowledgments

We would like to thank the NSF (grant number, CHE-1308211) and NASA (grant number, NNX14AI34G) for funding this work.

1.7 References

1. A. Zukauskas, A. Novickovas, P. Vitta, M. S. Shur, R. Gaska. "Raman Measurements in Water using a High-Power Light-Emitting Diode". J. Raman Spectrosc. 2003. 34: 471-473.

2. J. S. Greer. G. I. Petrov V. V. Yakovlev. "Raman Spectroscopy with LED Excitation Source". J. Raman Spectrosc. 2013. 44: 1058-1059

3. M. A. Schmidt. J. Kiefer. "Polarization-Resolved High-Resolution Raman Spectroscopy with a Light-Emittig Diode". J. Raman Spectrosc. 2013. 44: 1625-1627.

4. R. Adami, J. Kiefer. "Light-Emitting Diode Based Shifted-Excitation Raman Difference Spectroscopy (LED-SERDS)". Analyst. 2013. 138: 6258.

5. J. Kiefer. "Instantaneous Shifted-Excitation Raman Difference Spectroscopy (iSERDS)". J. Raman Spectrosc. 2014. 45: 980-983.

6. J.M. Harlander. Spatial Heterodyne Spectroscopy: Interferometric Performance at any Wavelength Without Scanning. [Ph.D. Thesis]. Madison, Wisconsin: The University of Wisconsin, 1991.

7. J. Harlander, R.J. Reynolds, F.L. Roesler. "Spatial heterodyne spectroscopy for the exploration of diffuse interstellar emission lines at far-ultraviolet wavelengths". Astrophys. J. 1992. 396: 730. 10.1086/171756.

8. N.R. Gomer, C.M. Gordon, P. Lucey, S.K. Sharma, J.C. Carter, S.M. Angel. "Raman Spectroscopy Using a Spatial Heterodyne Spectrometer: Proof of Concept". Appl. Spectrosc. 2011. 65(8): 849–857.

9. N. Lamsal, S.M. Angel. "Deep-Ultraviolet Raman Measurements Using a Spatial Heterodyne Raman Spectrometer (SHRS)". Appl. Spectrosc. 2015. 69(5): 525–534.

10. N. Lamsal, S. K. Sharma, T. E. Acosta, S. M. Angel. "Ultraviolet Stand-off Raman Measurements Using a Gated Spatial Heterodyne Raman Spectrometer". Appl. Spectrosc. 2016. 70 (4). 666-675.

11. J.M. Harlander, F.L. Roesler, S. Chakrabarti. Spatial heterodyne spectroscopy: a novel interferometric technique for the FUV. 1990. Pp. 120–131.

12. Strange, K. A.; Angel, S.M. “Transmission Raman Measurements using a Spatial Heterodyne Raman Spectrometer.” Appl. Spectrosc. In press

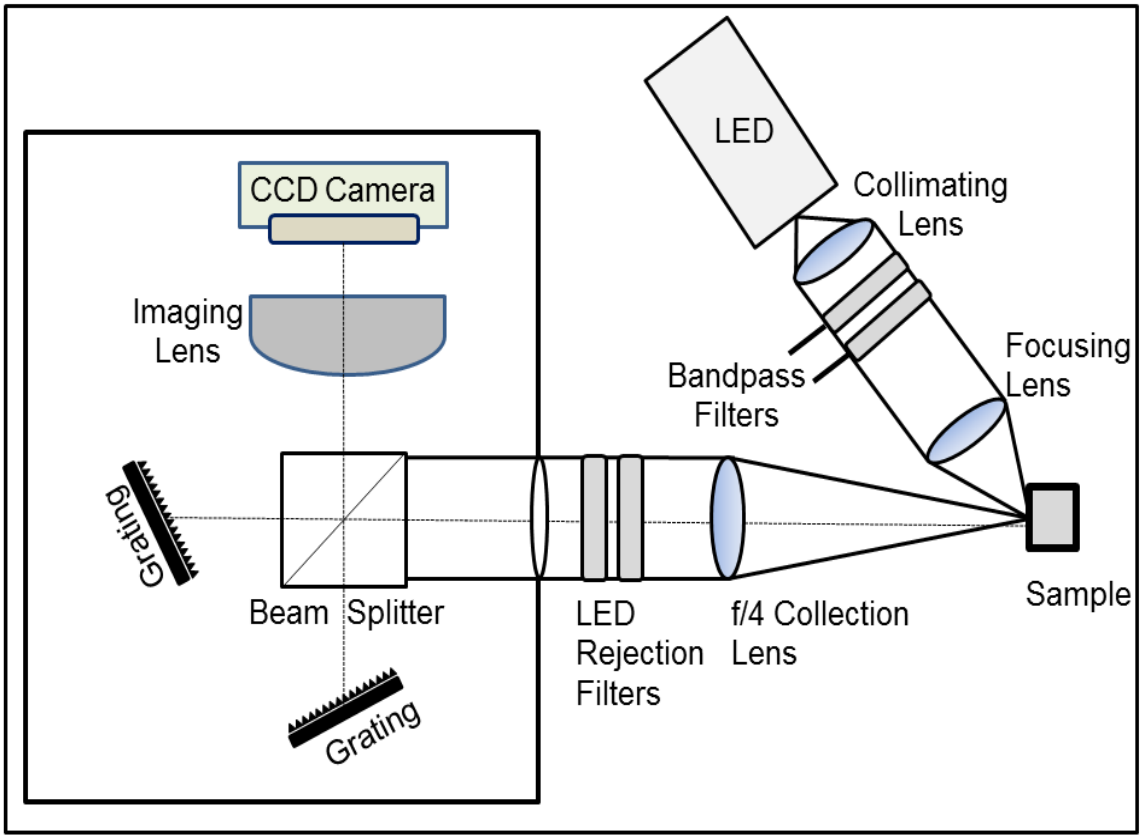

Figure 1.1. Detailed schematic of the spatial heterodyne Raman spectrometer layout for LED excitation. The sample is illuminated with the LED filtered through a 632.8 nm bandpass filter at approximately 45° with respect to the optical axis.

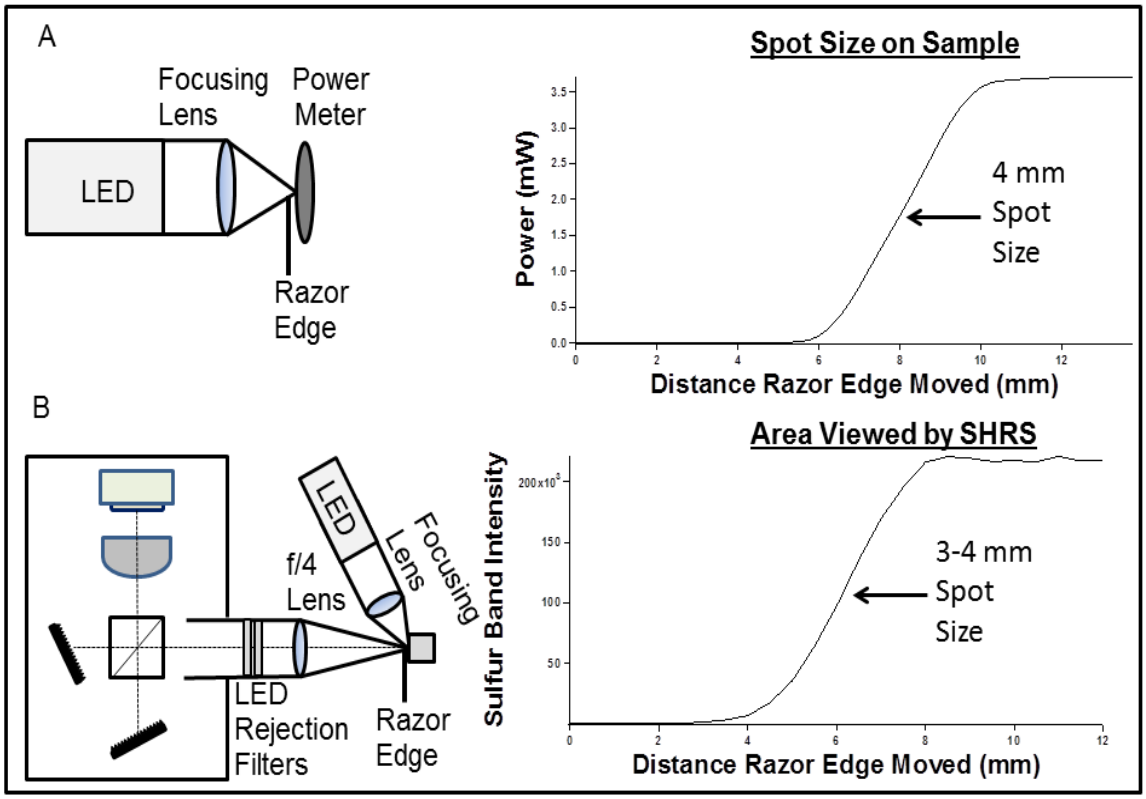

Figure 1.2.. Detailed schematic of experimental setup and results for determination of (A) LED spot size on sample and (B) area of LED spot viewed by SHRS.

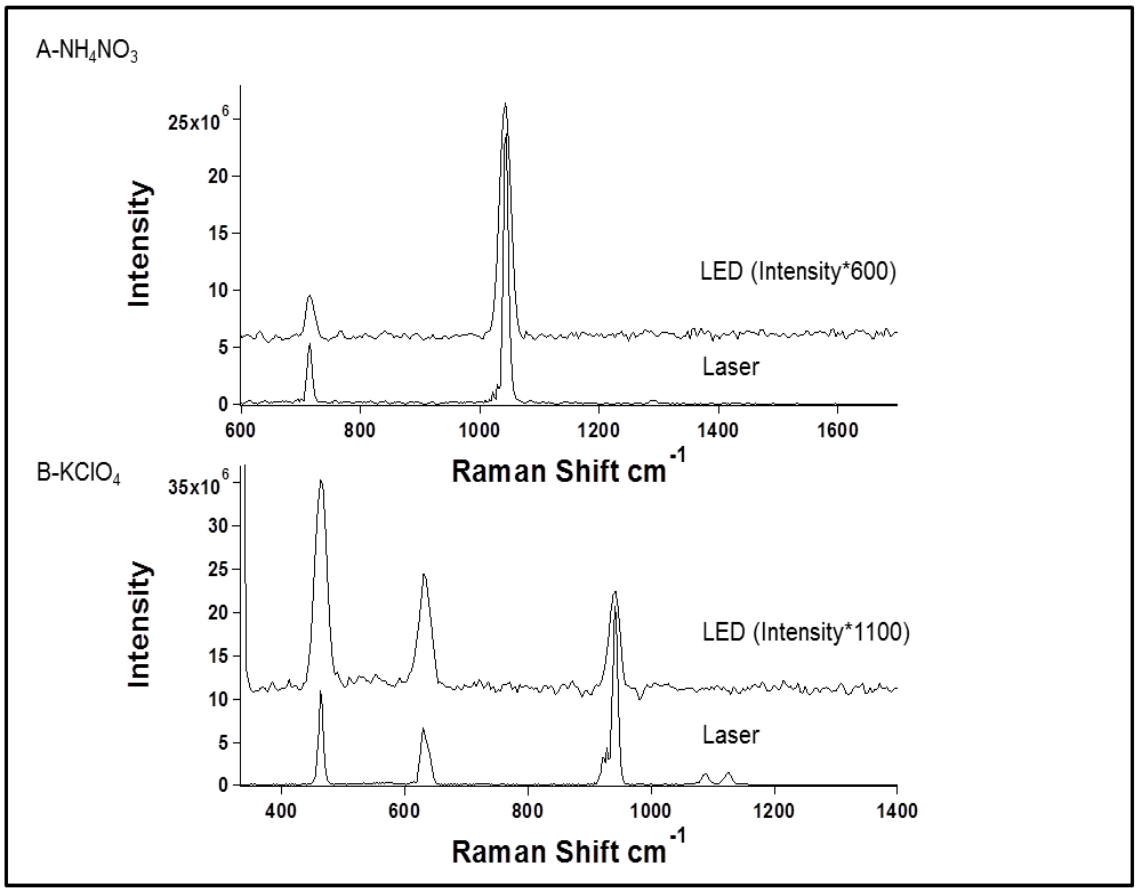

Figure 1.3. A comparison of LED and laser excitation. The laser spectra where collected with ~1 W of a 532 nm laser and a 10 s acquisition.[12] The LED spectra where collected with ~4 mW of a 632.8 nm LED and a 60 s acquisition time. The LED data intensities are multiplied in order to plot on the same graph using the same y-axis.

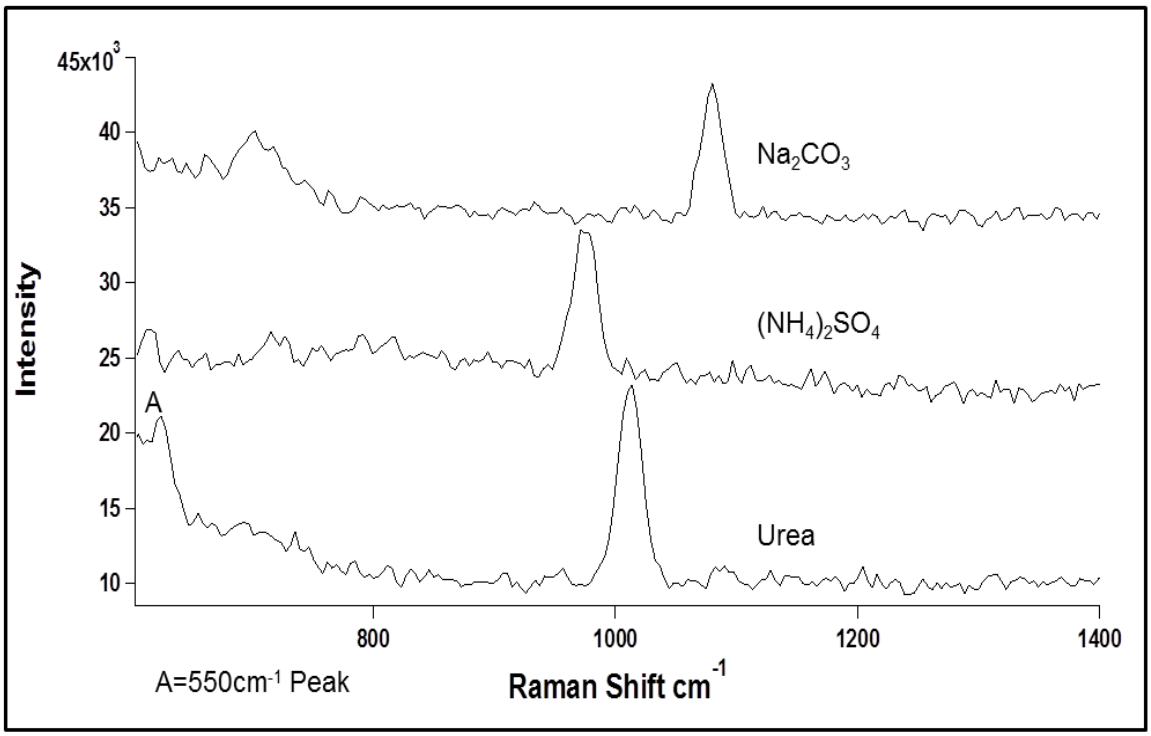

Figure 1.4. LED excited Raman spectra of some common solid samples. All spectra where collected with ~4 mW of 632.8 nm LED light at 60 s integration time with Littrow set to ~590 cm^{-1}. The peak labeled A is the 550 cm^{-1} line below the Littrow wavelength. Spectra are offset vertically for clarity.

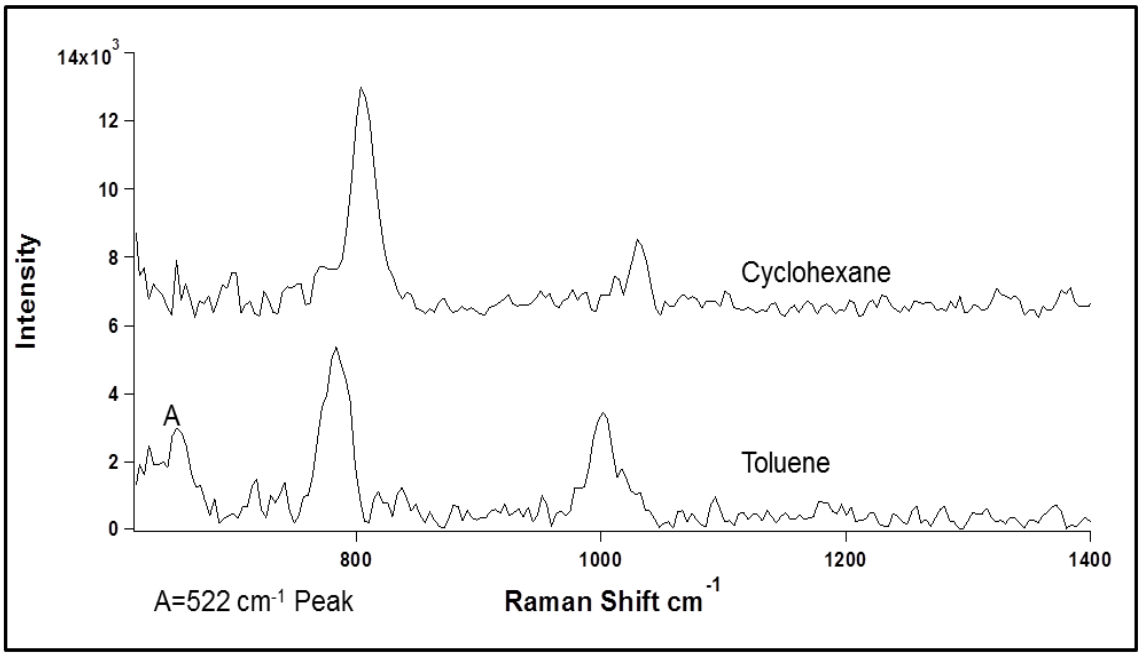

Figure 1.5. LED excited Raman spectra of some common liquid samples. All spectra where collected with ~4 mW of 632.8 nm LED light at 300 s integration time with Littrow set to ~590 cm^{-1}. The peak labeled A is the 522 cm^{-1} line from below the Littrow wavelength. Spectra are offset vertically for clarity

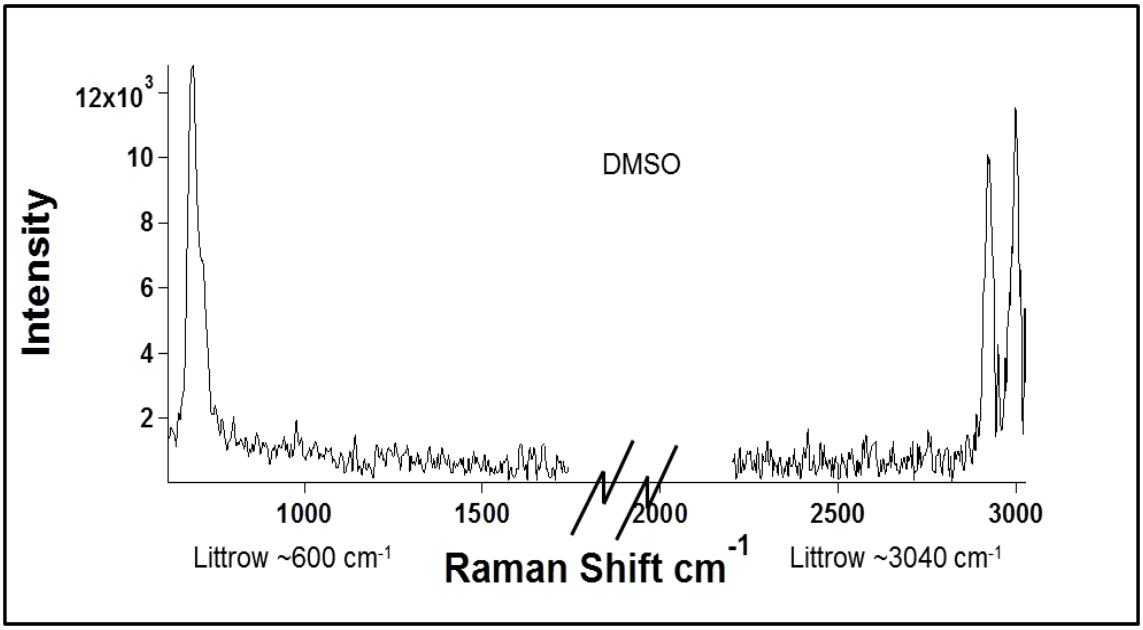

Figure 1.6. LED excited Raman Spectra of DMSO at two different Littrow positions. Both spectra where collected with ~4 mW of 632.8 nm LED light at 120 s integration time.

CHAPTER 2

Enhancement of Raman Signal for Gases Using Novel Optical Cells

2.1 Abstract

The analysis of gases using Raman spectroscopy is difficult due to the low molecular density. In previous work we demonstrated 10-20 fold enhanced Raman signals for gas measurements using a special type of hollow wave guide (HWG) developed by coating the inside of a hollow capillary cell with silver. The multipass capillary cell (MCC) provides enhanced Raman signals by increasing the interaction volume between the laser and the gas inside the cell[1-2]. The advantages of the MCC are easy alignment and simple construction. However the MCC has a relatively large diameter (3-5 mm) making it difficult to efficiently collect the light propagated in the MCC through the slit of a monochromator. Current work will show two separate projects that hope to further the effectiveness of MCCs. The first is exploring the use of a spatial heterodyne Raman spectrometer (SHRS) for use with large diameter MCCs. The SHRS's large acceptance angle, wide field of view, and the absence of a narrow slit is well suited to measuring large MCCs that would provide more signal enhancement due to a larger internal volume. The first part of this study will show preliminary data using a SHRS to measure gases in 3 and 5 mm diameter MCCs. Although in these early measurements the signal to noise ratio is still slightly lower than using a dispersive Raman spectrometer,

because of high background signals in the MCC devices used and imperfect filtering in the MCC, improvements are expected by the use of better background filtering in the SHRS. The second part of this study focuses on substrate-integrated hollow waveguides (iHWG) developed by Dr. Chance Carter's group at Lawrence Livermore National Laboratory.[3-4]

2.2 Introduction

Homonuclear gases like hydrogen, nitrogen, and oxygen are important industrial and environmental samples that cannot be measured with infrared spectroscopy. Many applictions like remote atmospheric measurements, and combustion analysis, are under conditions where sampling and physical contact is not possible.[5]. Raman is well established for measuring these types of samples and is a technique that requires no sample preperation and is well suited for in-situ analyses. The low molecular density of gases however leads to low Raman signals. Enhanced Raman cells have been demonstrated and include multipass optical cell that reflect and refocus the Raman excitation many times throughout the samples and liquid core waveguides that use an index of refraction difference to meet the condition of total internal reflection to guide the Raman excitation source through a large volume of sample, increasing the Raman signal.[6-12] The multipass cells tend to be bulky and easily misaligned limiting their effectiveness, while the liquid core waveguides will not work with gas samples because the index of refraction of gases is much too low to allow for total internal reflection.

A simple multipass capillary cell (MCC) design has been shown by Pearman et. al. that behaves like a combination of a mulitpass cell and a liquid core waveguide[1-2]. The laser light is reflected throughout the gas many times providing a signal

enhancement from the increased volume of sample excited. Unlike a traditional multipass cell the alignment is easy and stable. The MCC has shown to provide up to 15 fold enhancements but is limited due to Raman scattered light exiting the MCC with a very large numerical aperture. While a fiber optic is typically used to collect the light it comes with its own problems with light loss because of numerical aperture matching issues with the MCC. A better approach may be to directly couple the MCC to a newly developed Raman spectrometer known as the spatial heterodyne Raman spectrometer which has a very large field of view.

The SHRS is based on a stationary diffraction grating, heterodyne interferometer first introduced by Harlander and later modified by Gomer et al. for visible Raman measurements.[13-15] There is no entrance slit to limit light entering the spectrometer and the resolution is not strongly tied to aperture size. Heterodyning in the interferometer allows for high spectral resolution to be achieved with a relatively small number of samples, fixed by the number of horizontal pixels on the imaging detector. The large entrance aperture and wide acceptance angle provides high light throughput and allows large spots sizes to be used on the sample without light loss or the loss of spectral resolution. This is a key feature that will allow for the MCCs to be coupled to the spectrometer with large diameter optical fibers, or large bundles of fibers.

A newly designed substrate-integrated hollow waveguide (iHWG) will be used in this study. With the iHWG a channel is machined into a substrate, in our case Al, which will be used to propagate the excitation laser or sample signal through an increased volume of sample while maintaining a relatively small footprint. The channel in our case

is straight in order to capitalize on the laser reflection in a manner identical to the MCC, but more exotic shapes have been developed for use with mid-Infrared gas sensing.[3-4]

.

2.3 Experimental

Figure 2.1 is a detailed schematic for the gas Raman setup. A 532 nm (OEM MLLH) diode pumped laser set at ~200 mW power is reflected by a silvered mirror into the custom made MCC. The MCCs are hollow capillary tubes coated with a commercial silver coating solution purchased from Angel Gilding, Inc. The light is collected with a 25 mm diameter f/6 lens and collimated. The collimated beam passes through a 600 band pass filter (Andover 600FS40-25) and enters the SHRS where it is separated into the arms of the SHRS by a 25 mm beamsplitter (Thor Labs, CM1-BS013) onto a 25 mm, 150 grooves/mm grating. The gratings are imaged with a magnification of ~1 onto a liquid nitrogen cooled charge-coupled detector (CCD) with 1024x256 pixel (Princeton Instrument, Model LN/CCD-1024EUV), using a 86 mm focal length camera lens (Nikon AF Nikkor). CCD fringe images were recorded using Winspec software provided with the detector. Apart from the fringe image, three additional images were acquired for each spectrum. These additional images were sometimes used for background correction of the fringe images. Fourier transforms of the fringe images were performed using the fast Fourier transform (FFT) function in Matlab. Each spectrum was apodized using a Hamming function to reduce ringing effects in the spectral baseline. The Raman spectra were calibrated by locating the position of known Raman bands and using a polynomial fit. No flat field or instrument efficiency corrections, phase correction, smoothing,

sharpening, or any other post-processing such as zero filling was used for any of the data presented in this paper.

Figure 2.2 depicts the custom gas cell experimental setup used. A 532 nm laser (Spectra Physics Millenia) is focused into a fiber optic Raman probe. The fiber optic Raman probe is a 20 @ 1 setup with 20 collection fibers around a single laser guidance fiber. The 18 collection fibers are arranged linearly and coupled to a Kaiser Holospec f/1.8i spectrometer with a 25-micron slit and a charged coupled device (Princeton Instruments Pixis 400B). The spectra were taken using WinSpec/32 software. The probe end of the fiber optic Raman probe is coupled to a custom plate designed to interface with the new gas chamber. The Raman probe is then connected to a newly developed iHWG that rests on a platform. In this study multiple iHWGs were used.

Figure 2.3 is a detailed look at the multiple iHWGs used in this study. Fig. 2.3A is an iHWG with a protective Al coating applied to the channel in order to improve the percentage of reflected light thereby increasing the signal enhancement. There are no diffusion holes to expedited gas flow into the channel. Fig. 2.3B is an iHWG with an uncoated channel but has 5 diffusion holes to improve gas flow into the iHWG. The idea is to improve gas flow and potentially improve the system response time when a change in atmosphere occurs. Fig. 2.3C is an iHWG with an uncoated channel nearly double the length of the previous iHWGs and has no diffusion holes. These three iHWGs will be used under the same conditions to determine the enhancement factor each provides.

2.4 Results and Discussion

2.4.1 Gas Raman Measurements using the SHRS

Figure 2.4 shows the comparison of ambient N_2 gas collected using the experimental setup shown in Fig. 2.1 and the Fig. 2.2 with the gas chamber replaced with the MCCs. The Kaiser data is collected with 125 mw of 532 nm excitation with 20 accumulations with 3 s acquisition. The SHRS data uses 200 mw of 532 nm excitation with a 60 s acquisition. Fig. 2.4A shows the results collected using a 3 mm inner diameter MCC. The SHRS signal intensity is multiplied by a factor of 30 so both spectra can be plotted together. In this case the SHRS results are very similar with the Kaiser results but the SHRS results have a lower signal to noise ratio. The results shown with the 3 mm inner diameter MCC are on par with published results using the MCC. As the MCC inner diameter is increased however the SHRS is expected to outperform the Kaiser because of the much larger angle viewed by the SHRS. Fig. 2.4B shows the results using a 5 mm inner diameter MCC. The SHRS intensity data is multiplied by a factor of 10 in order to plot both on the same graph. When comparing the data the signal strength and noise of the SHRS is much higher while the signal to noise is lower. The noise levels in the data collected with the SHRS is quite high, likely due to the alignment of the collection lens and the MCC with the SHRS as well as the SHRS collecting excess light caused by the uncoated portion of the MCC. Improvement in the coating technique and improved alignment and baffling should provide better results.

2.4.2 Comparing the new iHWGs

Figure 2.5 shows the comparison of the response of the 3 new iHWG. The three iHWGs were used under similar conditions measuring ambient N_2. The N_2 peak intensity is calculated with each of the iHWGs and then ratioed with the signal peak intensity of ambient N_2 taken with no iHWG in place. The ratio gives a value known as the enhancement that is used to determine how well the iHWG performs. iHWG A has a signal enhancement of 40 which is much larger than achieved in the previous MCC studies.[1-2] iHWG B has a signal enhancement of around 13 which is lower than anticipated especially when it is the same size as iHWG A. iHWG B most likely performs so poorly because the channel is uncoated thereby limiting how well the walls propagate the signal, and the diffusion holes may be contributing negatively to propagation of signal down the channel. iHWG C has an enhancement of around 18. This value is in line with what is expected after measuring the enhancement of the uncoated iHWG B. The increased length is expected to cause an increase in the enhancement due to an increased volume of sample. The study shows that a coating of protected Al on the channel of the waveguide provides a drastic increase in the enhancement factor and this is an aspect of the iHWG design that future iterations should incorporate.

2.5 Conclusions

The Multipass Capillary Cell (MCC) provides enhanced Raman signals of gases up to 15-fold.[1-2] The large field of view and large acceptance angle of the SHRS allows the use of large MCCs, up to ~5 mm, which help to limit coupling losses while large

coupling losses are unavoidable using a dispersive spectrometer because of the small size of the spectrometer slit. The MCCs currently show relatively large background and this limits the sensitivity of the SHRS MCC measurement. Future work will focus on reducing background signals in the SHRS and the use of fiber optic coupling with the MCC. The new iHWGs return results that are on par or better than what has been achieved with the current use of the MCCs. The protected Al coating improved the iHWG response drastically when compared to uncoated iHWGs. The study gives a sense of the direction for further development of the iHWGs.

2.6 Acknowledgments

Special thanks to NSF for funding a portion of this research under CHE-1308211 and CHE 0526821 as well as Dr. Chance Carter and Lawrence Livermore National Laboratory.

2.7 References

1. W.F. Pearman, J.C. Carter, S. M. Angel, J.W-J. Chan. “Multi-pass capillary cell for enhanced Raman measurements of gases”. Appl. Spectrosc. 2008. 62. 285-289.
2. W.F. Pearman, J.C. Carte, S. M. Angel, J.W-J. Chan G. Herzberg. “Quantitative measurments of CO2 and CH4 using a multipass Raman capillary cell”. Appl Opt. 2008. 47. 4627-4632.
3. A. Wilk, J. C. Carter, M. Chrisp, A. M. Manuel, P. Mirkarimi, J.B. Alameda, B. Mizaikoff. “Substrate-Integrated Hollow Waveguides: A New Level of Integration in Mid-Infrared Gas Sensing”. Anal. Chem. 2013. 85. 11205-11210.
4. J. C. Carter, M. P. Chrisp, A. M. Manuel, B. Mizalkoff, A. Wilk, S. Kim. “SUBSTRATE-INTEGRATED HOLLOW WAVEGUIDE SENSORS”
5. G. Herzberg. Infrared and Raman spectra of Polyatomic Molecules (Van Nostrand Reinhold, New York, NY, 1945).
6. S. M. Adler-Golden, N. Goldstein, F. Bien, M.W. Mathew, M.E. Gersh, W.K. Cheng, F.W. Adams. “Laser Raman sensor for measurement of trace-hydrogen gas’. Appl. Opt. 1992. 31. 831-835.
7. W.R. Trutna, R.L. Byer. “Multiple-pass Raman gain cell”. Appl. Opt. 1980. 19. 301
8. R. A. Hill, A.J. Mulac, C.E. Hackett. “Retroreflecting multipass cell for Raman scattering”. Appl. Opt. 1977. 16. 2004-2006.
9. G.E. Walrafen, J. Stone. “Intensification of Spontaneous Raman Spectra by Use of Liquid core Optical Fibers”. Appl. Spectrosc. 1972. 26. 585.
10. G.E. Walrafen. “New Slitless Optical Fiber Laser-Raman Spectrometer”. Appl. Spectrosc. 1975. 29. 179
11. R. Altkorn, I. Koev, R.P. Duyne, M. Litorja. “Low-loss liquid-core optical fiber for low-refractive-index liquids: fabrication, characterization, and application in Raman spectroscopy”. Appl. Opt. 1997. 36. 8992
12. M. J. Pelletier, R. Altkorn. “Raman Sensitivity Enhancement for Aqueous Protein Samples Using a Liquid-Core Optical-Fiber Cell”. Anal. Chem. 2001. 73. 1393.
13. J.M. Harlander. Spatial Heterodyne Spectroscopy: Interferometric Performance at any Wavelength Without Scanning. [Ph.D. Thesis]. Madison, Wisconsin: The University of Wisconsin, 1991.
14. J. Harlander, R.J. Reynolds, F.L. Roesler. “Spatial heterodyne spectroscopy for the exploration of diffuse interstellar emission lines at far-ultraviolet wavelengths”. Astrophys. J. 1992. 396: 730. 10.1086/171756.

15. N.R. Gomer, C.M. Gordon, P. Lucey, S.K. Sharma, J.C. Carter, S.M. Angel. "Raman Spectroscopy Using a Spatial Heterodyne Spectrometer: Proof of Concept". Appl. Spectrosc. 2011. 65(8): 849–857.

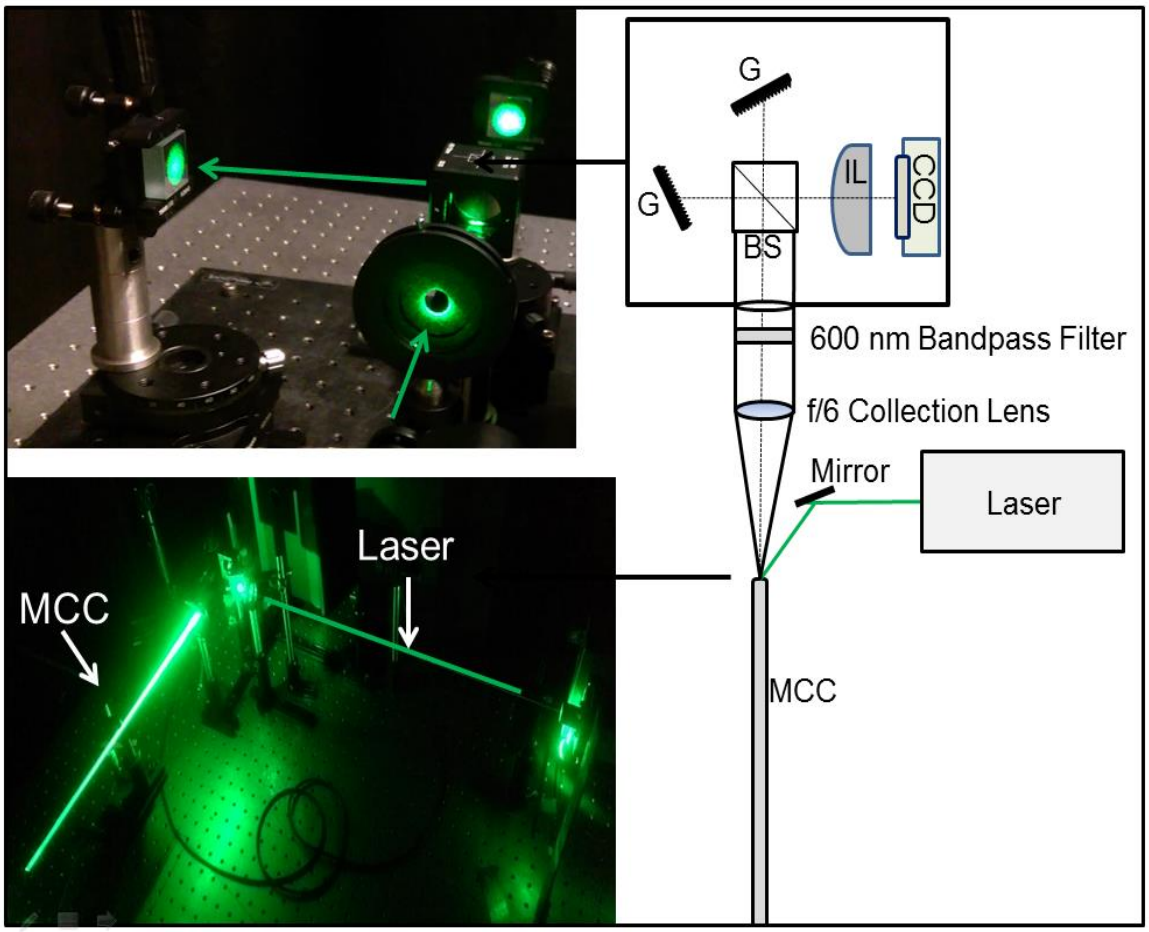

Figure 2.1. Detailed schematic of the gas Raman SHRS instrument setup. grating (G); beamsplitter (BS); imaging lens (IL); charge-coupled device (CCD). A 532 nm laser is used at ~10° from the optical axis to illuminate the interior of the multipass capillary cell.

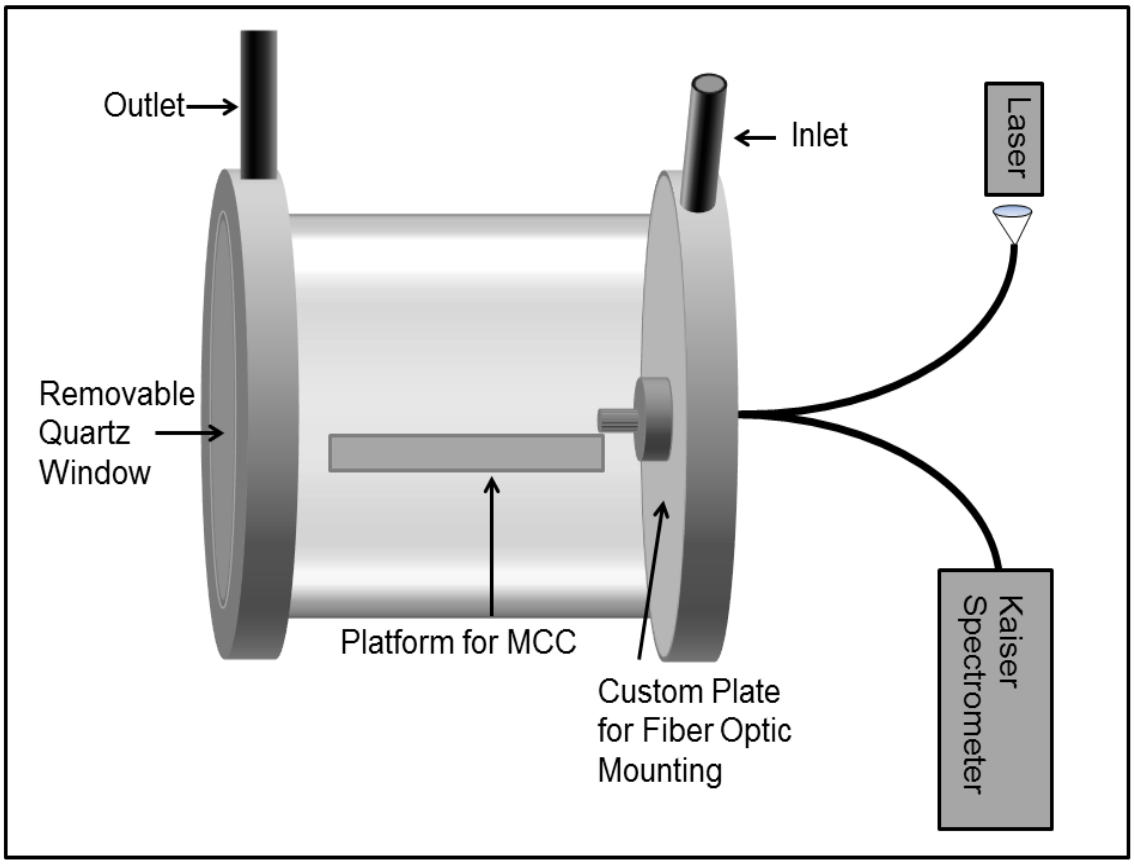

Figure 2.2. A detailed schematic of the custom gas cell N_2 Raman setup used. The laser and Kaiser spectrometer are coupled to a fiber optic Raman probe that connects though the wall of a newly designed gas chamber to a iHWG. The gas cell is enlarged to show details.

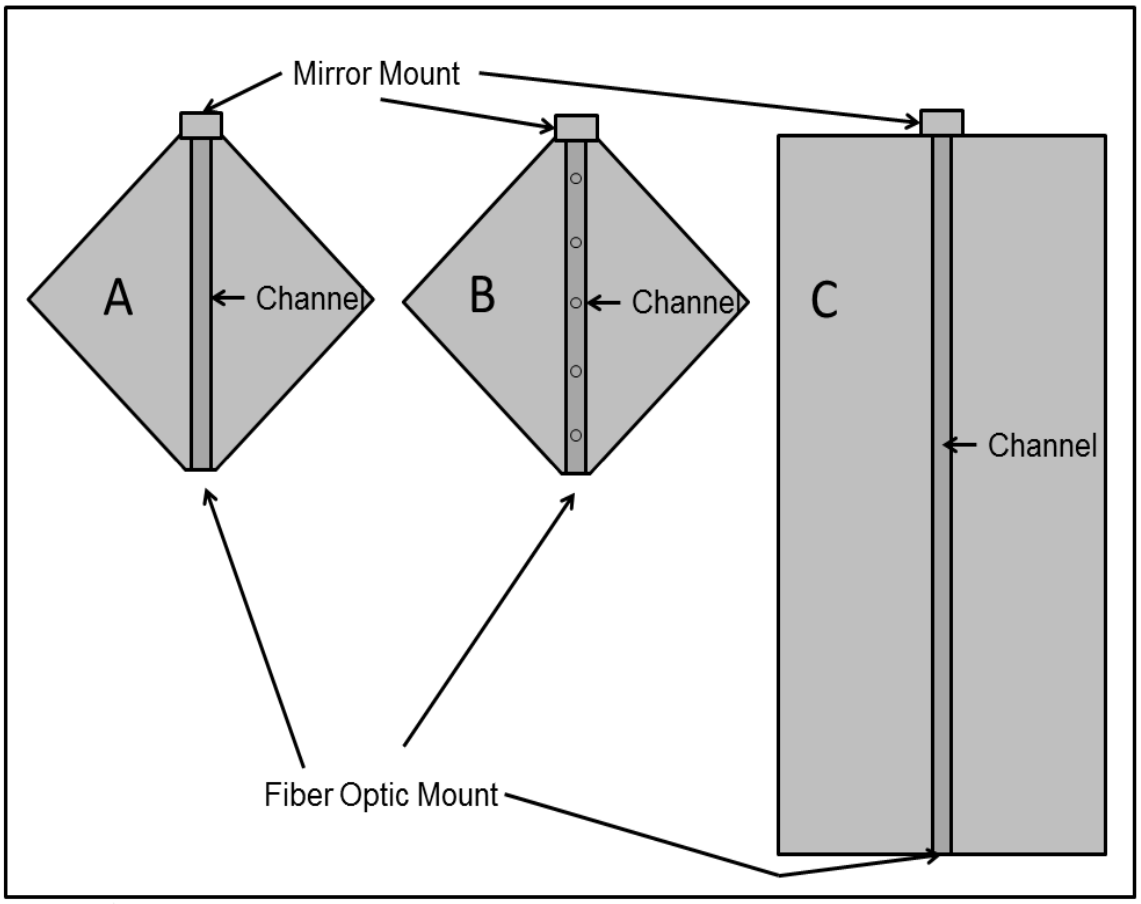

Figure 2.3. The 3 newly designed iHWGs are precision machined from Aluminum. iHWG A has a protected Al coated channel 58 mm long with no diffusion holes, iHWG B has an uncoated channel 58 mm long with 5 diffusion holes, iHWG C has an uncoated channel 100 mm long with no diffusion holes.

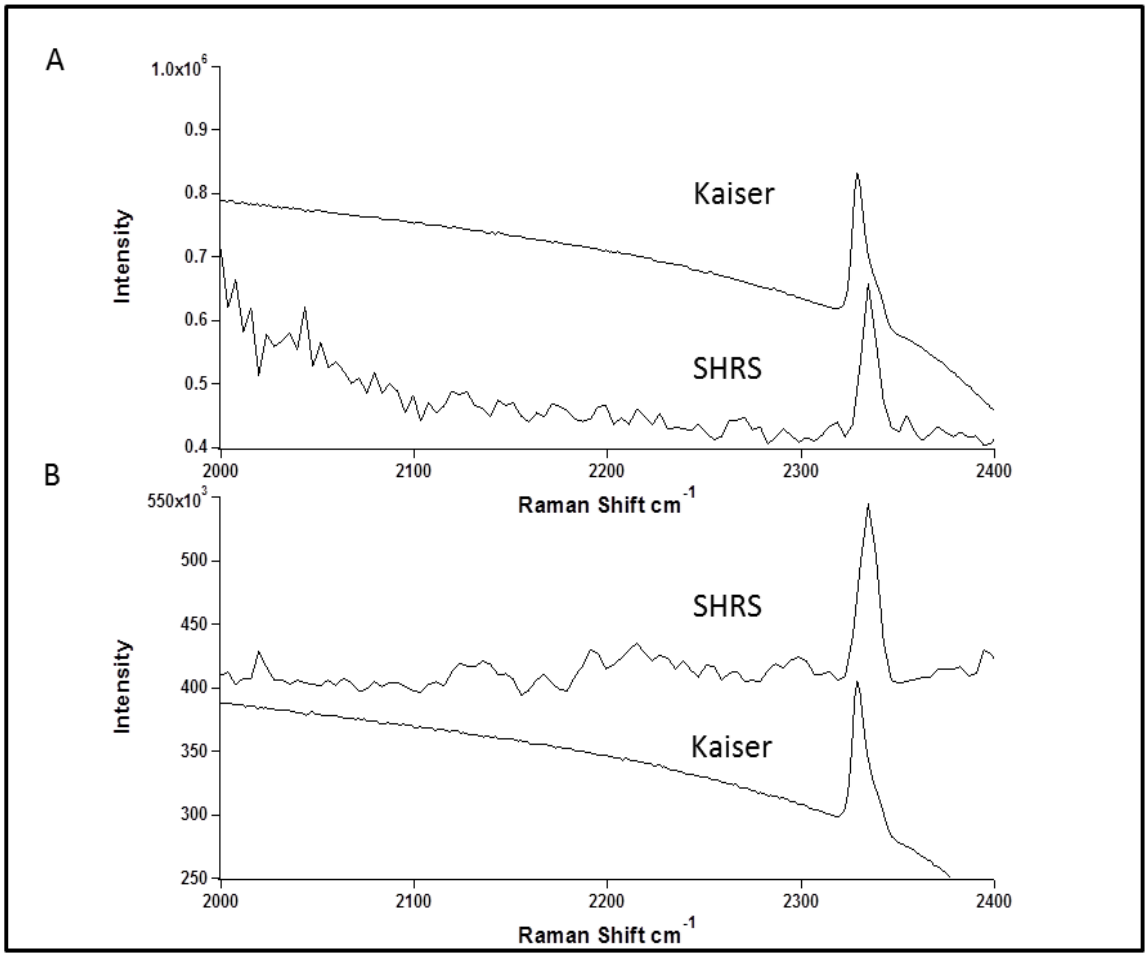

Figure 2.4. A comparison of ambient N_2 Raman spectra collected with the SHRS versus the Kaiser holospec at different capillary sizes. A) is the spectra collected using a 3 mm inner diameter MCC while, B) is the spectra collected using a 5 mm inner diameter MCC. SHRS data is offset and intensity multiplied for clarity.

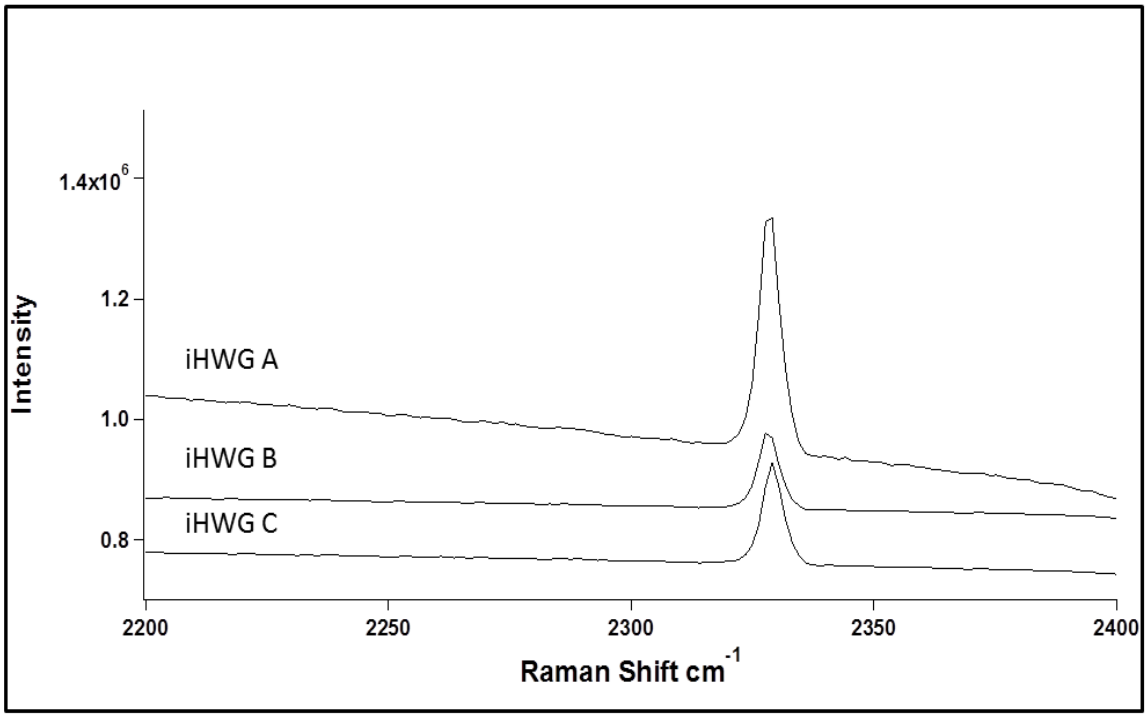

Figure 2.5. A comparison of the 3 new iHWGs. All spectra are of ambient N_2 collected using a 532 nm laser at various power levels with a 60 s acquisition time. iHWG A uses 121 mW, iHWG B uses 121 mW, and iHWG C uses 114 mW of Laser power. iHWG B and iHWG C are offset for clarity.

REFERENCES

1. A. Wilk, J. C. Carter, M. Chrisp, A. M. Manuel, P. Mirkarimi, J.B. Alameda, B. Mizaikoff. “Substrate-Integrated Hollow Waveguides: A New Level of Integration in Mid-Infrared Gas Sensing”. Anal. Chem. 2013. 85. 11205-11210.

2. A. Zukauskas, A. Novickovas, P. Vitta, M. S. Shur, R. Gaska. “Raman Measurements in Water using a High-Power Light-Emitting Diode”. J. Raman Spectrosc. 2003. 34: 471-473.

3. G.E. Walrafen, J. Stone. “Intensification of Spontaneous Raman Spectra by Use of Liquid core Optical Fibers”. Appl. Spectrosc. 1972. 26. 585.

4. G.E. Walrafen. “New Slitless Optical Fiber Laser-Raman Spectrometer”. Appl. Spectrosc. 1975. 29. 179.

5. G. Herzberg. Infrared and Raman spectra of Polyatomic Molecules (Van Nostrand Reinhold, New York, NY, 1945).

6. J. C. Carter, M. P. Chrisp, A. M. Manuel, B. Mizalkoff, A. Wilk, S. Kim. “SUBSTRATE-INTEGRATED HOLLOW WAVEGUIDE SENSORS”

7. J. Harlander, R.J. Reynolds, F.L. Roesler. “Spatial heterodyne spectroscopy for the exploration of diffuse interstellar emission lines at far-ultraviolet wavelengths”. Astrophys. J. 1992. 396: 730. 10.1086/171756.

8. J. Kiefer. “Instantaneous Shifted-Excitation Raman Difference Spectroscopy (iSERDS)”. J. Raman Spectrosc. 2014. 45: 980-983.

9. J.M. Harlander, F.L. Roesler, S. Chakrabarti. Spatial heterodyne spectroscopy: a novel interferometric technique for the FUV. 1990. Pp. 120–131.

10. J.M. Harlander. Spatial Heterodyne Spectroscopy: Interferometric Performance at any Wavelength Without Scanning. [Ph.D. Thesis]. Madison, Wisconsin: The University of Wisconsin, 1991.

11. J. S. Greer. G. I. Petrov V. V. Yakovlev. “Raman Spectroscopy with LED Excitation Source”. J. Raman Spectrosc. 2013. 44: 1058-1059

12. M. A. Schmidt. J. Kiefer. “Polarization-Resolved High-Resolution Raman Spectroscopy with a Light-Emittig Diode”. J. Raman Spectrosc. 2013. 44: 1625-1627.

13. M. J. Pelletier, R. Altkorn. “Raman Sensitivity Enhancement for Aqueous Protein Samples Using a Liquid-Core Optical-Fiber Cell”. Anal. Chem. 2001. 73. 1393.
14. N. Lamsal, S. K. Sharma, T. E. Acosta, S. M. Angel. “Ultraviolet Stand-off Raman Measurements Using a Gated Spatial Heterodyne Raman Spectrometer”. Appl. Spectrosc. 2016. 70 (4). 666-675.

15. N. Lamsal, S.M. Angel. “Deep-Ultraviolet Raman Measurements Using a Spatial Heterodyne Raman Spectrometer (SHRS)”. Appl. Spectrosc. 2015. 69(5): 525–534.

16. N.R. Gomer, C.M. Gordon, P. Lucey, S.K. Sharma, J.C. Carter, S.M. Angel. “Raman Spectroscopy Using a Spatial Heterodyne Spectrometer: Proof of Concept”. Appl. Spectrosc. 2011. 65(8): 849–857.

17. R. Adami, J. Kiefer. “Light-Emitting Diode Based Shifted-Excitation Raman Difference Spectroscopy (LED-SERDS)”. Analyst. 2013. 138: 6258.

18. R. A. Hill, A.J. Mulac, C.E. Hackett. “Retroreflecting multipass cell for Raman scattering”. Appl. Opt. 1977. 16. 2004-2006.

19. R. Altkorn, I. Koev, R.P. Duyne, M. Litorja. “Low-loss liquid-core optical fiber for low-refractive-index liquids: fabrication, characterization, and application in Raman spectroscopy”. Appl. Opt. 1997. 36. 8992

20. S. M. Adler-Golden, N. Goldstein, F. Bien, M.W. Mathew, M.E. Gersh, W.K. Cheng, F.W. Adams. “Laser Raman sensor for measurement of trace-hydrogen gas’. Appl. Opt. 1992. 31. 831-835.

21. Strange, K. A.; Angel, S.M. “Transmission Raman Measurements using a Spatial Heterodyne Raman Spectrometer.” Appl. Spectrosc. In press

22. W.F. Pearman, J.C. Carte, S. M. Angel, J.W-J. Chan G. Herzberg. “Quantitative measurments of CO2 and CH4 using a multipass Raman capillary cell”. Appl Opt. 2008. 47. 4627-4632.

23. W.F. Pearman, J.C. Carter, S. M. Angel, J.W-J. Chan. “Multi-pass capillary cell for enhanced Raman measurements of gases”. Appl. Spectrosc. 2008. 62. 285-289.

24. W.R. Trutna, R.L. Byer. “Multiple-pass Raman gain cell”. Appl. Opt. 1980. 19.